Available online at www.sciencedirect.com
ScienceDirect
Polymer 48 (2007) 1047–1057
polymer
www.elsevier.com/locate/polymer

Morphology and properties of nanocomposites formed from ethylene/methacrylic acid copolymers and organoclays

Rhutesh K. Shah[1], Do Hoon Kim, D.R. Paul*

Department of Chemical Engineering and Texas Materials Institute, The University of Texas at Austin, Austin, TX 78712, USA

Received 15 December 2006; received in revised form 27 December 2006; accepted 2 January 2007
Available online 8 January 2007

Abstract

Nanocomposites were prepared by melt mixing ethylene/methacrylic acid copolymers and organoclays, which were compared to equivalent composites prepared from low-density polyethylene (LDPE) and a sodium ionomer of poly(ethylene-*co*-methacrylic acid). The effects of matrix modification and organoclay structure on the morphology and properties of these nanocomposites were evaluated using stress–strain analysis, wide-angle X-ray scattering (WAXS), and transmission electron microscopy coupled with particle analysis. With all four polymers, the use of a two-tailed organoclay, $M_2(HT)_2$, led to the formation of more exfoliated nanocomposites than a one-tailed organoclay, $M_3(HT)_1$. Nanocomposites prepared from ethylene/methacrylic acid copolymers revealed better exfoliation compared to similar composites prepared from LDPE. It seems that the presence of relatively small quantities (1.3–3.1 mol%) of the polar methacrylic acid monomer aids in improving the organoclay exfoliation efficiency of these polymers. Nanocomposites prepared from the sodium ionomer of poly(ethylene-*co*-methacrylic acid) exhibited the highest levels of organoclay exfoliation compared to all other polymers examined in this study. However, from the observations made in this study, it was not possible to determine conclusively the relative interaction of carboxyl acid groups versus the salt form with the organoclay and, thus, their influence on exfoliation; additional studies will be needed to reach a conclusion on this important point.

Keywords: Nanocomposite; Polyethylene; Poly(ethylene-*co*-methacrylic acid)

1. Introduction

Nanocomposites prepared by melt mixing organically modified montmorillonite clays (organoclays) and polyolefins continue to generate much commercial interest because of their potential for significant improvements in thermal, mechanical, barrier, and flammability properties at low-filler levels. In order to generate the high-aspect ratio particles required for the aforementioned improvements it is necessary to exfoliate the montmorillonite platelets in the polymer matrix. This is difficult particularly in polyolefins, since there are no favorable interactions between the non-polar polymer and the polar aluminosilicate clays. Although complete exfoliation of clay particles in melt processed polyolefin nanocomposites has not been reported to date, it is possible to prepare nanocomposites with commercially acceptable levels of organoclay dispersion by employing an appropriate organoclay in conjunction with some degree of chemical modification of the polymer matrix. Grafting of maleic anhydride on the polyolefin backbone is known to significantly improve the interactions between polyolefins and organoclays, and thus, improve exfoliation [1–5]. In fact, the use of maleic anhydride grafted polypropylene as a compatibilizer has led to numerous applications for polypropylene–organoclay nanocomposites in the automotive industry [6–8]. Other approaches to improve polyolefin–organoclay compatibility include surface treatment of the polyolefin particles [9] and copolymerization of the olefin monomer with a polar monomer like acrylic acid [10] or vinyl acetate [11–15].

* Corresponding author. Tel.: +1 512 471 5392; fax: +1 512 471 0542.
E-mail address: drp@che.utexas.edu (D.R. Paul).
[1] Present address: School of Engineering and Applied Sciences (SEAS), Harvard University, Cambridge, MA 02138, USA.

0032-3861/$ - see front matter © 2007 Elsevier Ltd. All rights reserved.
doi:10.1016/j.polymer.2007.01.002

In this work we describe the preparation of nanocomposites from copolymers of ethylene and the polar methacrylic acid monomer. In addition, nanocomposites were also made from an ionomer prepared by neutralizing some of the acid groups of an ethylene/methacrylic acid copolymer [16]. The levels of organoclay exfoliation achieved in these nanocomposites were compared to that in an equivalent composite prepared from low-density polyethylene (LDPE). All composites examined in this study were prepared by melt mixing the polymers and organoclays in a twin-screw extruder. The effects of matrix modification and organoclay structure on the morphology and properties of the nanocomposites were evaluated using stress–strain analysis, wide-angle X-ray scattering (WAXS), and transmission electron microscopy coupled with particle analysis.

2. Experimental

2.1. Materials

The polymers used in this study are listed in Table 1. These include commercially available grades of poly(ethylene-*co*-methacrylic acid), a sodium ionomer of poly(ethylene-*co*-methacrylic acid), and a comparable grade of LDPE. For brevity, in this manuscript, poly(ethylene-*co*-methacrylic acid) will be referred to as ''EMAA'' and the sodium ionomer of poly(ethylene-methacrylic acid) will be referred to simply as ''ionomer''. The four polymers were chosen such that they had similar melt indices. This was done to eliminate the effects of differences in melt viscosities on organoclay exfoliation [17]. Ethylene/methacrylic acid copolymers with two different acid concentrations (EMAA-1 and EMAA-2) were used to evaluate the effects of the content of the polar comonomer on the organoclay exfoliation efficiency of the polymers. The ionomer selected had the same concentration of unneutralized methacrylic acid (~9 wt%) as EMAA-2 with ~6 wt% of neutralized methacrylic acid.

Organically modified clays were generously donated by Southern Clay Products and were used as received. They were prepared by a cation exchange reaction between sodium montmorillonite (Na-MMT) and quaternary ammonium surfactants [18]. The surfactants selected for preparing the organoclays include one with a single long-alkyl tail, $M_3(HT)_1$ (trimethyl hydrogenated tallow), and another with two long-alkyl tails, $M_2(HT)_2$ (dimethyl bis(hydrogenated tallow)). A nomenclature system, similar to that used in prior papers [18,19], has been adopted to describe the amine structure in a concise manner, i.e., M for methyl, H for hydrogen, and HT for hydrogenated-tallow oil, which consists predominantly (~61%) of C_{18} chains [20]. The organoclays, thus, allowed us to explore the effect of the number of alkyl tails on the extent of organoclay exfoliation in the four polymers chosen for this study. Selected properties of these organoclays are also included in Table 1.

2.2. Melt processing

Melt compounded composites were prepared using a Haake, co-rotating, intermeshing twin-screw extruder (diameter = 30 mm, $L/D = 10$) using a barrel temperature of 200 °C, a screw speed of 280 rpm, and a feed rate of 1200 g/h. The polymers were dried in a vacuum oven at 65 °C for a minimum of 48 h prior to compounding while the organoclays were used as received. These two components were premixed and fed into the extruder using a single hopper.

Table 1
Materials used in this study

Materials (abbreviation used in this study)	Commercial designation	Specifications	Supplier
Low-density polyethylene (LDPE)	LD 621	Density = 0.92 g/cc MI = 1.9 g/10 min	Exxon Mobil Chemical Company
Ethylene/methacrylic acid copolymer (EMAA-1)	Nucrel® 0403	Density = 0.93 g/cc MI = 3.2 g/10 min Methacrylic acid content = 3.9 wt%	E. I. du Pont de Nemours and Company
Ethylene/methacrylic acid copolymer (EMAA-2)	Nucrel® 0903	Density = 0.93 g/cc MI = 2.6 g/10 min Methacrylic acid content = 8.9 wt%	
Sodium ionomer of ethylene/methacrylic acid copolymer (Ionomer)	Surlyn® 8945	Density = 0.96 g/cc MI = 4.5 g/10 min Methacrylic acid content = 15.2 wt% Sodium content = 1.99 wt% Neutralization = ~40%	
Organoclay: trimethyl hydrogenated-tallow ammonium montmorillonite ($M_3(HT)_1$)	Experimental	Organic loading[a] = 95 MER Organic content = 29.6 wt% d_{001} spacing[b] = 18 Å	Southern Clay Products
Organoclay: dimethyl bis(hydrogenated tallow) ammonium montmorillonite ($M_2(HT)_2$)	Cloisite® 20A	Organic loading[a] = 95 MER Organic content = 39.6 wt% d_{001} spacing[b] = 25.5 Å	

[a] The organic loading describes the number of milliequivalents of amine salt used per 100 g clay (MER) during the cation exchange reaction with sodium montmorillonite.

[b] The basal spacing corresponds to the characteristic Bragg reflection peak d_{001} obtained from a powder WAXS scan of the organoclay.

Tensile specimens (ASTM D638) were prepared by injection molding using an Arburg Allrounder 305-210-700 injection-molding machine using a barrel temperature of 220 °C, mold temperature of 45 °C, injection pressure of 40 bar, and a holding pressure of 40 bar. After molding, the samples were immediately sealed in a polyethylene bag and placed in a vacuum desiccator for a minimum of 24 h prior to testing.

2.3. Testing and characterization

Tensile tests were conducted at room temperature according to ASTM D696 using an Instron model 1137 machine equipped with digital data acquisition capabilities. Modulus was measured using an extensiometer at a crosshead speed of 0.51 cm/min. Elongation at break and the ultimate tensile strength were measured at a crosshead speed of 5.1 cm/min. In most cases, the stress–strain curves did not reveal a distinct yield point; hence, that data are not included in this paper. Typically, data from six specimens were averaged to determine the tensile properties with standard deviations of the order of 1–7% for modulus, 1–3% for tensile strength at break, and 1–5% for elongation at break.

WAXS was conducted using a Scintag XDS 2000 diffractometer in the reflection mode with an incident X-ray wavelength of 1.542 Å (Cu Kα radiation) at a scan rate of 1.0° per minute. X-ray analysis was performed at room temperature on injection-molded Izod bars. The specimens were oriented such that the incident beam reflected off the major face. Samples for TEM analysis were taken from the core portion of an Izod bar parallel to the flow direction but perpendicular to the major face. Ultrathin sections ~50 nm in thickness were cut with a diamond knife at a temperature of −65 °C using a RMC PowerTome XL microtome. Sections were collected on 300 mesh grids and subsequently dried with filter paper. These were then examined using a JEOL 2010F TEM equipped with a field emission gun at an accelerating voltage of 120 kV. The negative films containing the electron micrographs were

Table 2
Mechanical properties deduced from stress–strain experiments on the unfilled polymers and their nanocomposites

Polymer	Organoclay	Clay content (MMT, wt%)	Tensile modulus (E, MPa)	Relative modulus (E/E_m)	Ultimate tensile strength (5.1 cm/min, MPa)	Elongation at break (5.1 cm/min, %)
LDPE	None	0.0	114	1.00	13.6	108
	$M_3(HT)_1$	2.5	155	1.36	14.4	87
		5.0	172	1.51	14.4	80
		7.5	194	1.70	14.1	73
		10	218	1.91	14.0	67
	$M_2(HT)_2$	2.5	178	1.56	14.2	83
		5.0	227	1.99	14.3	77
		7.5	280	2.46	14.3	70
		10	375	3.29	14.2	62
EMAA-1	None	0.0	118	1.00	13.9	136
	$M_3(HT)_1$	2.5	151	1.31	14.3	120
		5.0	180	1.52	14.5	108
		7.5	220	1.86	14.9	99
		10	260	2.20	15.2	90
	$M_2(HT)_2$	2.5	189	1.60	14.7	111
		5.0	259	2.20	16.5	99
		7.5	328	2.78	17.5	91
		10	425	3.60	18.0	82
EMAA-2	None	0.0	73	1.00	15.4	185
	$M_3(HT)_1$	2.5	112	1.53	16.1	176
		5.0	133	1.82	16.7	165
		7.5	178	2.44	17.4	148
		10	220	3.01	18.5	133
	$M_2(HT)_2$	2.5	147	2.01	17.8	156
		5.0	203	2.78	19.1	143
		7.5	254	3.48	20.6	134
		10	353	4.83	22.2	120
Ionomer	None	0.0	262	1.00	21.3	194
	$M_3(HT)_1$	2.5	349	1.33	21.2	117
		5.0	410	1.56	21	111
		7.5	465	1.77	22.1	119
		10	563	2.15	23.2	116
	$M_2(HT)_2$	2.5	403	1.54	22.3	127
		5.0	560	2.14	23.8	111
		7.5	732	2.79	26.6	72
		10	919	3.51	29.4	65

electronically scanned and converted into gray scale tagged-image file format (TIFF) files. To conduct quantitative analysis on these images, the lengths, thicknesses, and aspect ratios of the particles were determined. The lengths and thicknesses of the dispersed platelets and agglomerates were traced digitally on an overlapped blank layer in Adobe Photoshop under high magnification. Two separate tracings were done for each TEM pictures: one contained the lengths of the particles and the other one contained their thicknesses. The resulting black and white layer files were then imported into an image analysis software, Sigmascan Pro, which analyzed the traced particles, assigned a numerical label to each of them, and exported their characteristic dimensions to a different file. In previous studies from this laboratory [9,19,21,22], the average particle aspect ratio for a given nanocomposite was determined by dividing the average particle length by the average particle thickness. In this study, an extra effort was taken to determine the aspect ratio of each individual particle by dividing its length by its thickness. Number-average and weight-average values of the aspect ratios determined using these two methods were later compared to the aspect ratios deduced from the Halpin–Tsai model for nanocomposites exhibiting similar levels of reinforcement.

3. Results

Mechanical properties deduced from stress–strain experiments on the unfilled polymers and their nanocomposites are tabulated in Table 2.

3.1. LDPE vs EMAA

Fig. 1 displays typical stress–strain diagrams of the nanocomposites prepared by melt mixing $M_2(HT)_2$ organoclay with LDPE and EMAA. Composites made using $M_3(HT)_1$ organoclay revealed similar trends, and hence are not shown here. For all samples, the stress–strain diagrams suggest the absence of a distinct yield point followed by different levels of strain hardening. The curves shift to higher stresses as the clay content increases – a result of progressive reinforcement as the clay content increases. It is noteworthy that while the stress–strain curves for the nanocomposites prepared from EMAA copolymers are widely spaced from each other, those for composites prepared from LDPE are not so well separated. In other words, upon increasing the MMT content from 2.5 wt% to 10 wt%, the increase in reinforcement of LDPE-based composites is not as significant as that for EMAA-based composites. This suggests that as the montmorillonite content increases from 2.5 wt% to 10 wt% in LDPE-based composites, the concentration of the high-aspect ratio particles does not increase as much as seen in EMAA-based composites.

Tensile modulus data for nanocomposites prepared by melt mixing LDPE and EMAAs with $M_3(HT)_1$ and $M_2(HT)_2$ organoclays are presented in Fig. 2(a). It is clear that for all three polymers the level of reinforcement achieved with the two-tailed organoclay, $M_2(HT)_2$, is significantly greater than that with the one-tailed organoclay, $M_3(HT)_1$. These trends

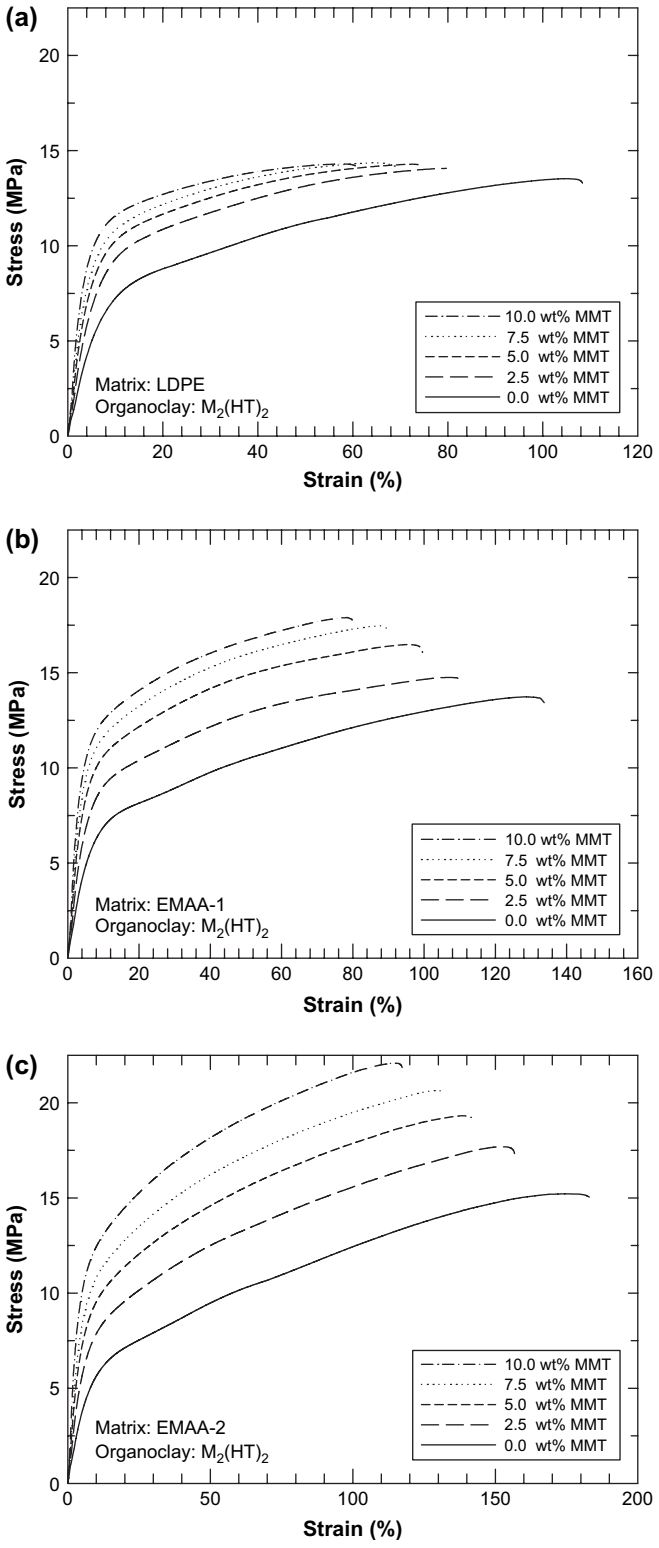

Fig. 1. Stress–strain diagrams of nanocomposites prepared from $M_2(HT)_2$ organoclay and (a) LDPE, (b) ethylene/methacrylic acid copolymer containing 3.9 wt% methacrylic acid (EMAA-1), and (c) ethylene/methacrylic acid copolymer containing 8.9 wt% methacrylic acid (EMAA-2). The crosshead speed was fixed at 5.1 cm/min.

are opposite from those reported for nanocomposites prepared from nylon 6 [18,23]. It appears that, unlike nylon 6, these polymers have more affinity for the largely aliphatic alkyl

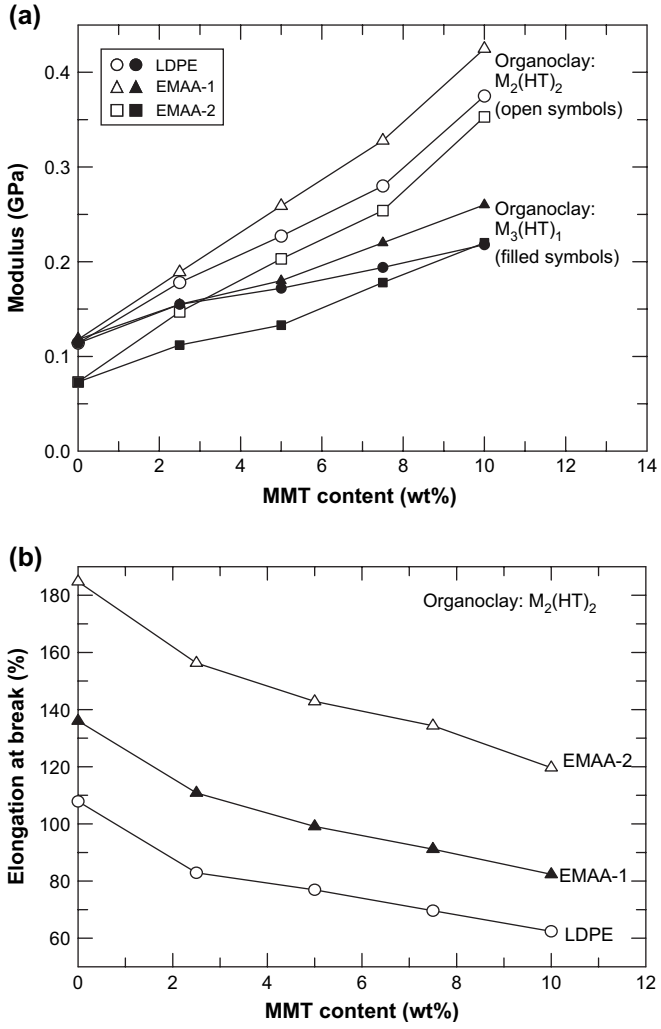

Fig. 2. Tensile modulus (a) and elongation at break (b) of nanocomposites prepared from LDPE and the two ethylene/methacrylic acid copolymers (EMAA-1 and EMAA-2).

tails than the polar surface of the aluminosilicate clays. The two-tailed surfactant not only offers a greater number of alkyl–polymer interactions compared to the one-tailed surfactant, but also shields the surface of the clay better than the latter. The combination of these effects results in a higher level of organoclay exfoliation, and thus, greater reinforcement in the nanocomposites prepared from $M_2(HT)_2$ organoclay compared to those prepared from $M_3(HT)_1$ organoclay. A comparison between the moduli of nanocomposites prepared from LDPE and EMAA-1 also provides some interesting insights into the relative levels of exfoliation in these systems. Despite the fact that the two unfilled polymers have very similar moduli, nanocomposites prepared from EMAA-1 exhibit higher levels of reinforcement compared to equivalent composites prepared from LDPE. This suggests higher levels of organoclay dispersion in nanocomposites prepared from EMAA-1 than those from LDPE.

The relationship between the MMT content of the $M_2(HT)_2$-based nanocomposites and the elongation at break is shown in Fig. 2(b). It is interesting to note the differences in the elongation at break for the three unfilled polymers. It appears that the ductility of these copolymers increases with an increase in the methacrylic acid content. This is likely a consequence of the lower crystallinity caused by the incorporation of the bulky methacrylic acid units [24]. As expected, the ductility of all polymers decreases with an increase in the MMT content. Nanocomposites prepared using $M_3(HT)_1$ organoclay show similar trends as shown in Table 2.

Fig. 3 shows TEM micrographs comparing the morphologies of nanocomposites prepared from LDPE and EMAA copolymers using $M_2(HT)_2$ organoclay. The concentration of montmorillonite in all three cases is 2.5 wt%. The micrographs of nanocomposites prepared from EMAA-1 and EMAA-2 reveal thinner clay stacks compared to the one prepared from LDPE, which suggest better clay dispersion in the former than in the latter. Note the differences in magnification as indicated by the lengths of the scale bars in the different views. A quantitative comparison of the level of organoclay exfoliation in the three matrices is provided in Section 4.

WAXS scans of injection-molded nanocomposite samples containing 2.5 wt% MMT prepared from LDPE and the two ethylene/methacrylic acid copolymers are shown in Fig. 4. It should be noted that the scans presented here primarily reflect the composite morphology in the skin of the injection-molded samples, which could be quite different from the core (due to

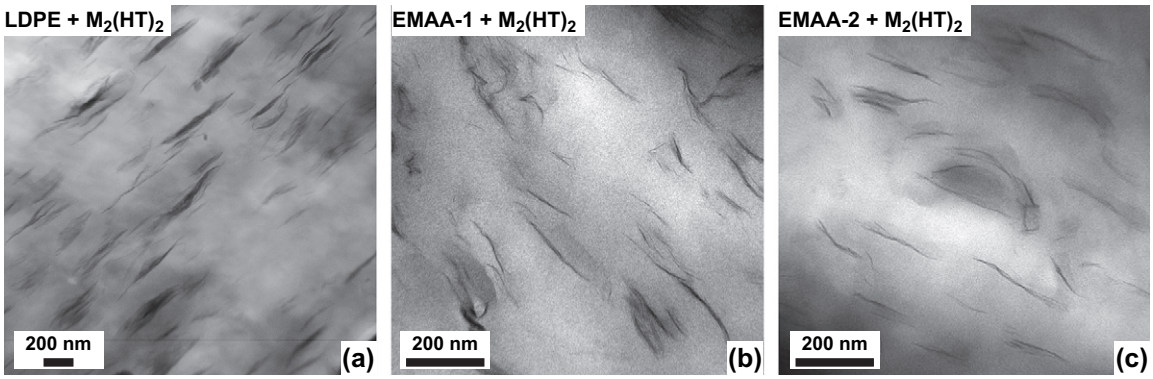

Fig. 3. TEM micrographs of nanocomposites prepared from $M_2(HT)_2$ organoclay and (a) LDPE, (b) ethylene/methacrylic acid copolymer containing 3.9 wt% methacrylic acid (EMAA-1), and (c) ethylene/methacrylic acid copolymer containing 8.9 wt% methacrylic acid (EMAA-2). The concentration of MMT in all cases is ~2.5 wt%.

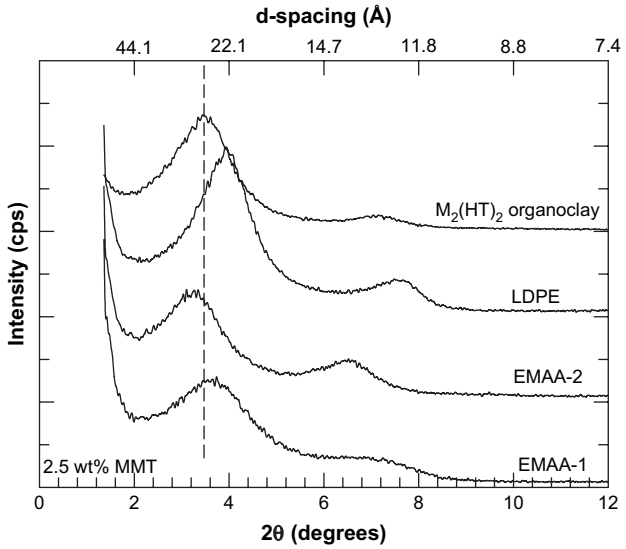

Fig. 4. WAXS scans of nanocomposites prepared from LDPE and the two ethylene/methacrylic acid copolymers (EMAA-1 and EMAA-2) and $M_2(HT)_2$ organoclay. The concentration of MMT in all cases is ~2.5 wt%. The X-ray scan of the $M_2(HT)_2$ organoclay is plotted for comparison and the dashed vertical line shows the position of its d_{001} peak. The curves are shifted vertically for clarity.

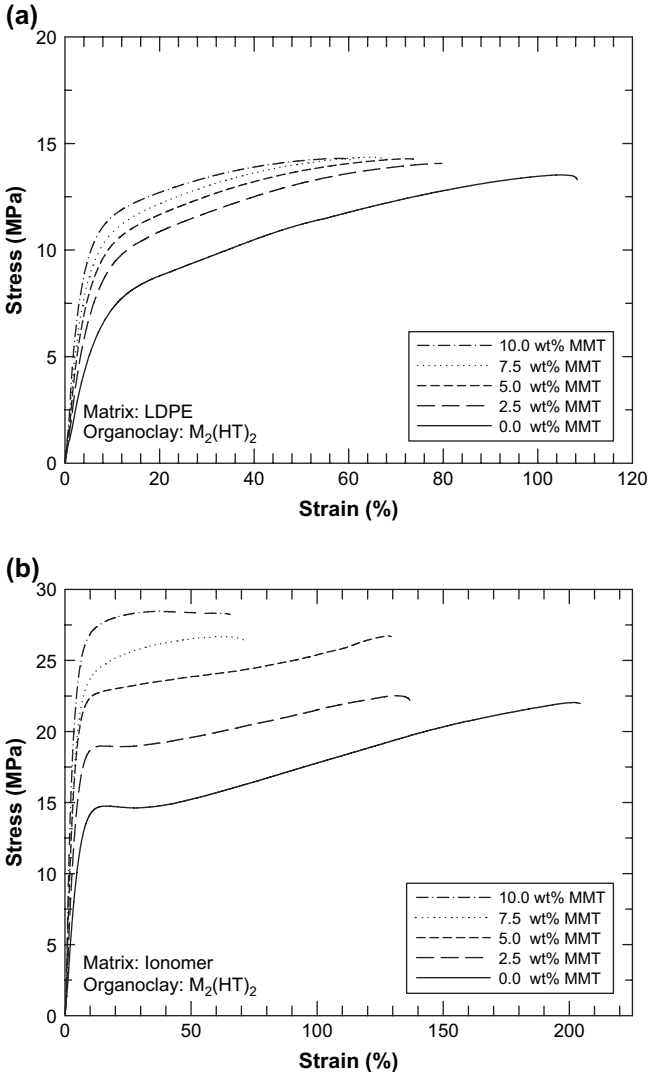

Fig. 5. Stress–strain diagrams of nanocomposites prepared from $M_2(HT)_2$ organoclay and (a) LDPE and (b) ionomer. The crosshead speed was fixed at 5.1 cm/min.

differences in platelet alignment caused by the flow fields during the injection-molding process) [1,25,26]. The X-ray scan for the neat $M_2(HT)_2$ organoclay is also included for comparison. The scans of all nanocomposites show a distinct peak indicative of the presence of unexfoliated tactoids. However, these peaks have shifted in different directions with respect to the peak in the WAXS pattern of the pristine $M_2(HT)_2$ organoclay. The position of the scattering peak for nanocomposites is dependent on several phenomena that transpire during melt processing. One of them is the reduction in *d*-spacing caused by the thermal degradation of the organoclay that occurs when nanocomposites are processed at a temperature of 200 °C. A detailed discussion on organoclay degradation in melt processed LDPE–$M_2(HT)_2$ and LDPE–$M_3(HT)_1$ nanocomposites was given in an earlier paper [27]. The other factor is the intercalation of the polymer and/or low-molecular weight oligomers (that may be present in the matrix) in the interplatelet region of the organoclay which results in an increase in its *d*-spacing. Recently other explanations have also emerged [27,28]. It appears that in the case of LDPE–$M_2(HT)_2$ composites the degradation effects dominate while in the case of EMAA-2-based nanocomposites the intercalation effects dominate.

3.2. LDPE vs ionomer

Typical stress–strain behavior of LDPE and the ionomer are compared in Fig. 5. The stress–strain curve for the unfilled ionomer, unlike that for LDPE, reveals a distinct yield point. It also reveals considerable degree of strain hardening, the extent of which gradually decreases with an increase in the montmorillonite content. Similar to the EMAA nanocomposites described earlier, the stress–strain curves for the ionomer are widely spaced compared to those for LDPE, suggesting a larger increase in the degree of reinforcement compared to LDPE when the montmorillonite content increases from 2.5 wt% to 10 wt%.

Tensile moduli of nanocomposites prepared from LDPE and the ionomer are compared in Fig. 6. Like the LDPE and EMAA nanocomposites, the ionomer–$M_2(HT)_2$ nanocomposites also exhibit a higher level of reinforcement compared to ionomer–$M_3(HT)_1$ nanocomposites. As an extension of this idea, a three-tailed organoclay, methyl trihexadecyl ammonium montmorillonite was also examined. This resulted in even higher levels of reinforcement in the two polymers [19,29]. The effect of the number of alkyl tails of the organic modifier on the level of organoclay exfoliation in the two polymers is corroborated by the pictorial evidence provided by the TEM micrographs in Fig. 7. For both polymers, the use of a multiple-tailed organoclay results in the formation of

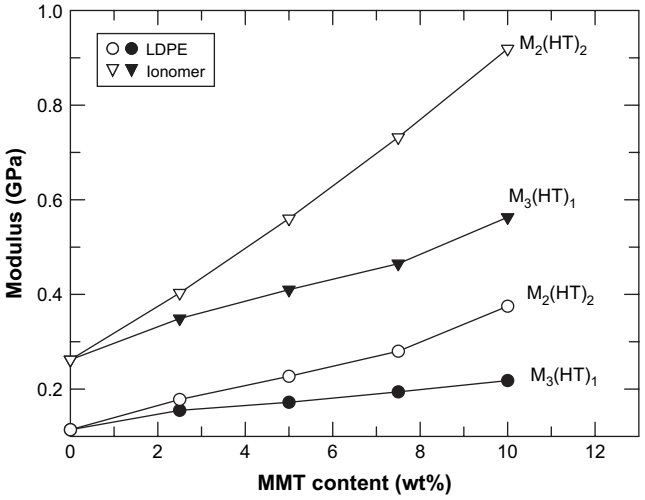

Fig. 6. Tensile modulus of nanocomposites prepared from (a) LDPE (b) and ionomer using $M_3(HT)_1$ (one tailed) and $M_2(HT)_2$ (two tailed) organoclays as a function of MMT content.

nanocomposites with more exfoliated morphology compared to equivalent composites prepared from a one-tailed organoclay. Another clear trend from the micrographs is that for both organoclays the level of exfoliation achieved in the ionomer is higher than that achieved in LDPE. It appears that the presence of the neutralized and unneutralized methacrylic acid groups and clusters of sodium ion in the ionomer improves the favorable interactions between the organoclay and the polymer, which subsequently leads to better exfoliation in these systems compared to nanocomposites prepared from LDPE.

The WAXS scans of nanocomposites prepared from LDPE and the ionomer are compared in Fig. 8. As mentioned earlier, the scans presented here primarily reflect the composite morphology in the skin of the injection-molded samples, which could be quite different from the core [1,19,25,26]. The X-ray scans of the organoclays are also included for comparison (dotted curves). For nanocomposites prepared from both LDPE and the ionomer, the X-ray peaks of the composites formed from the one-tailed organoclay, $M_3(HT)_1$, have shifted to lower *d*-spacings than the organoclay. This is largely due to the thermal degradation of the one-tailed surfactant as mentioned earlier [27]. WAXS scans of nanocomposites prepared from the two-tailed organoclay are different for LDPE and the ionomer. While the X-ray peak for the LDPE–$M_2(HT)_2$ composites shifted to lower *d*-spacings, the X-ray patterns of the ionomer–$M_2(HT)_2$ nanocomposites shifted to higher *d*-spacings relative to the peak for the $M_2(HT)_2$ organoclay. As mentioned earlier, the increase in the *d*-spacing observed

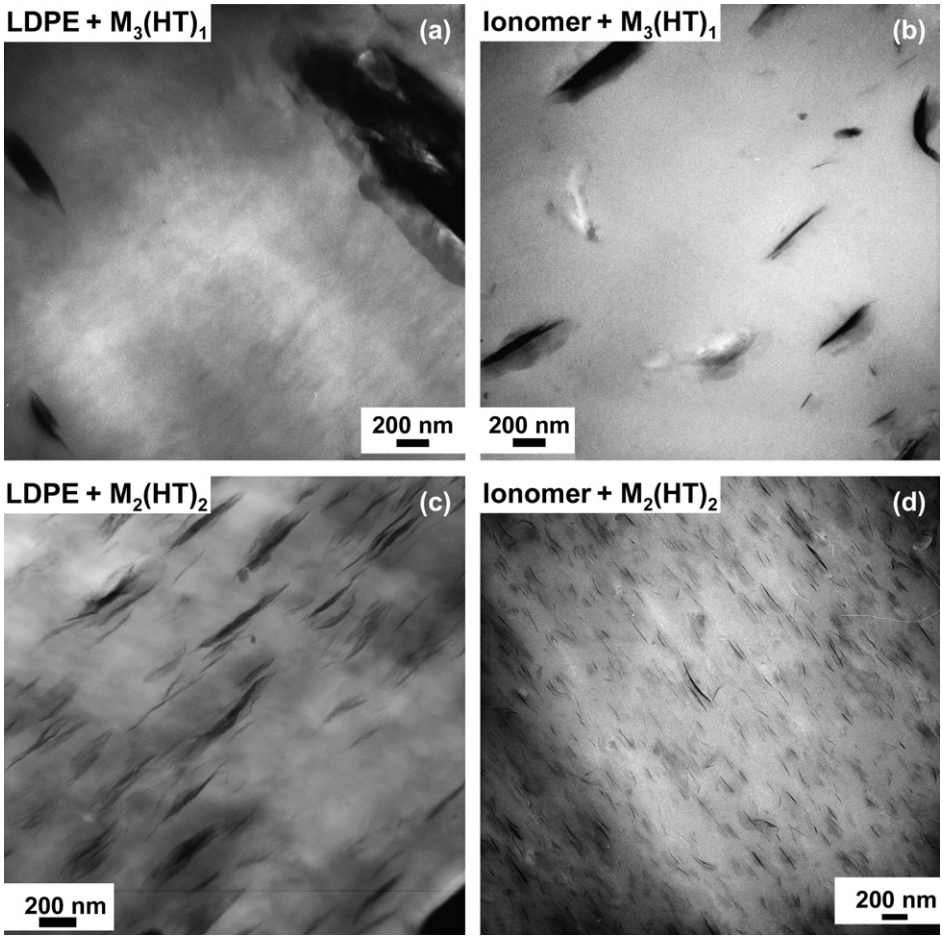

Fig. 7. TEM micrographs of nanocomposites prepared from LDPE and the ionomer using (a,b) a one-tailed organoclay, $M_3(HT)_1$, and (c, d) a two-tailed organoclay, $M_2(HT)_2$. The concentration of MMT in all four samples is ~2.5 wt%.

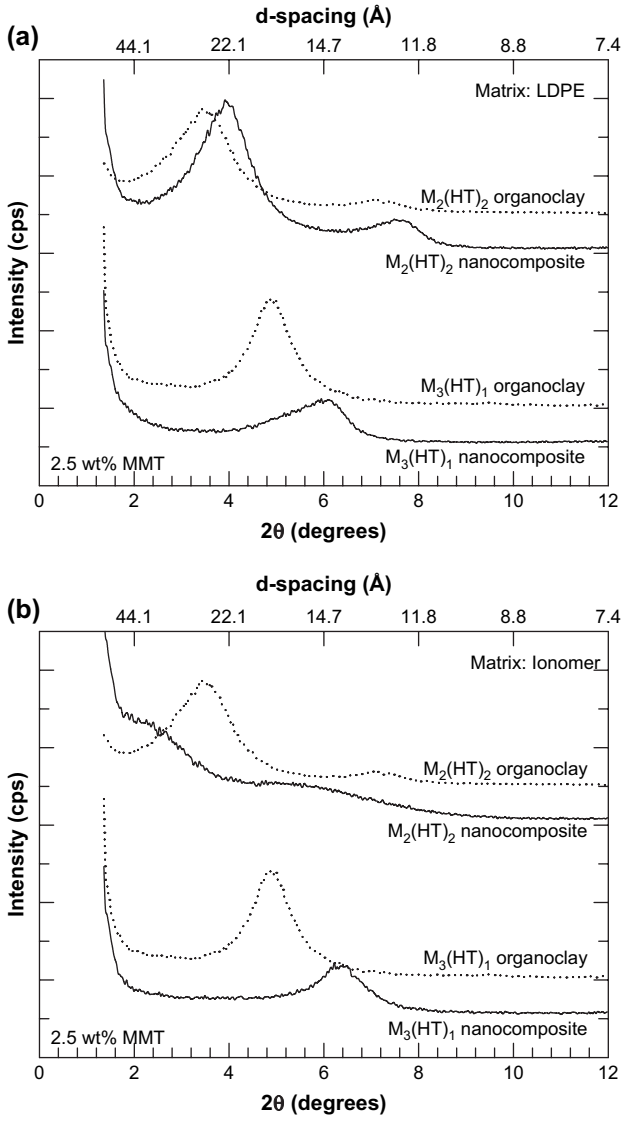

Fig. 8. WAXS scans of nanocomposites formed from (a) LDPE and (b) ionomer. The dotted curves are the X-ray scans of the corresponding organoclays and are plotted for comparison. The curves are shifted vertically for clarity.

in the ionomer–$M_2(HT)_2$ nanocomposites could be a result of the intercalation of the polymer or some oligomers (that may be present in the polymer) inside the clay galleries. The position of the peak was independent of the montmorillonite concentration of the nanocomposites [29,30].

4. Discussion

As described above, nanocomposites were prepared by melt mixing organoclays with ethylene/methacrylic acid copolymers and a sodium ionomer of poly(ethylene-*co*-methacrylic acid). Although, all of the above three polymers exfoliated the organoclays more effectively than the base polyolefin (LDPE), the level of exfoliation was lower than that exhibited by nylon 6-based composites [21]. In terms of preference for a surfactant treatment, all four polymers showed the same trend, i.e., unlike nylon 6 [18,23], these polymers exfoliate

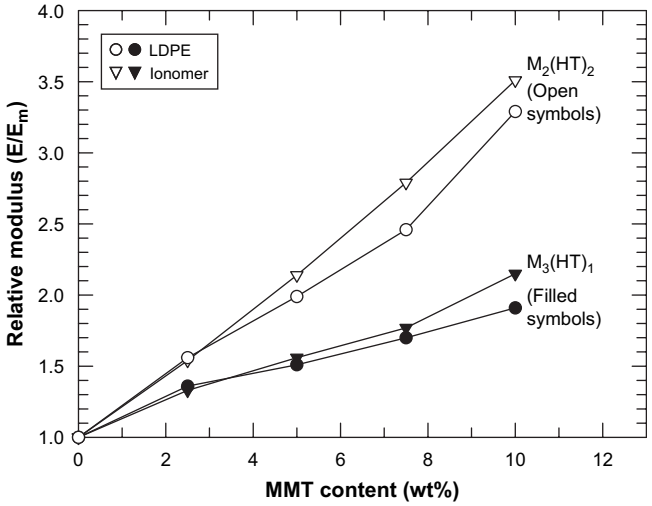

Fig. 9. Relative modulus of nanocomposites prepared from LDPE and the ionomer using $M_3(HT)_1$ and $M_2(HT)_2$ organoclays versus MMT content.

the two-tailed organoclay, $M_2(HT)_2$, much better than the one-tailed organoclay, $M_3(HT)_1$ (see Figs. 3 and 7). It would be interesting to see if this trend is reversed (becomes similar to nylon 6) if the methacrylic acid content of the copolymer is increased beyond a certain critical concentration. However, such an investigation is beyond the scope of this paper and should be the focus of another study.

A quantitative comparison of the relative levels of exfoliation achieved in all of the above polymers could shed further light on the effects of matrix modification on organoclay exfoliation. Generally, relative modulus data (E/E_m) are a reliable measure of the level of exfoliation when comparing nanocomposites made from polymers that have similar moduli (e.g., LDPE and EMAA-1). However, this measure is inadequate, and sometimes misleading, while comparing nanocomposites prepared from polymers whose modulus values differ considerably from each other [30,31]. For example, as described earlier and shown in Fig. 7, nanocomposites (containing 2.5 wt% MMT) prepared from the ionomer display a significantly more exfoliated morphology compared to equivalent composites prepared from LDPE. However, as shown in Fig. 9, composites prepared from these two polymers exhibit similar levels of reinforcement (relative modulus) with either organoclays. The fact that the modulus of the ionomer is more than twice that of LDPE contributes somewhat to this effect. Composite theory [32,33] predicts that for a given filler aspect ratio, low-modulus matrices offer greater potential for reinforcement by a given amount of filler than high-modulus matrices due to the larger ratio of filler modulus to matrix modulus.

Alternatively, a comparison of the filler aspect ratios in different nanocomposites should provide useful insights into the relative levels of organoclay exfoliation of these systems. As described in Section 2, number-average and weight-average aspect ratios of nanocomposites containing 2.5 wt% MMT were computed using two different methods. These values are tabulated in Table 3. As an example, histograms of MMT particle lengths, thicknesses, and aspect ratios of nanocomposites

Table 3
Results of particle analysis of nanocomposites

	Total number of particles	Number-average particle length ($\overline{\ell_n}$, nm)	Weight-average particle length ($\overline{\ell_w}$, nm)	Number-average particle thickness ($\overline{t_n}$, nm)	Weight-average particle thickness ($\overline{t_w}$, nm)	Number-average aspect ratio $\langle \ell/t \rangle_n$	Weight-average aspect ratio $\langle \ell/t \rangle_w$	$(\overline{\ell_n}/\overline{t_n})$	$(\overline{\ell_w}/\overline{t_w})$
LDPE + 2.5 wt% MMT	166	181	224	20.9	35.7	13	18	9	6
EMAA-1 + 2.5 wt% MMT	321	122	167	5.5	10.1	26	34	22	17
EMAA-2 + 2.5 wt% MMT	290	140	166	6.4	10.1	28	36	22	16
Ionomer + 2.5 wt% MMT	334	118	138	3.7	4.9	36	44	32	28

containing ~2.5 wt% MMT prepared from EMAA-1 and $M_2(HT)_2$ organoclay are presented in Fig. 10. The underlying assumptions in this approach are that the samples are homogeneous and the snapshot views provided by the TEM micrographs are representative of the morphology of the entire composite sample. The data in Table 3 suggest that the filler particles in the nanocomposites prepared from EMAA-1, EMAA-2, and the ionomer are shorter and thinner than the ones in the LDPE nanocomposites. To get a clear picture of the effect of matrix modification on organoclay exfoliation in LDPE-based composites a plot of the number-average particle aspect ratio of the nanocomposites, $\langle \ell/t \rangle_n$, is plotted as a function of the methacrylic acid content of the matrix polymers in Fig. 11. The choice of $\langle \ell/t \rangle_n$ for the above-mentioned graph was arbitrary since all four averages revealed similar trends. Of the four nanocomposites, the one prepared from LDPE has the lowest average aspect ratio. The incorporation of methacrylic acid seems to increase the ability to exfoliate the organoclays as shown by the higher aspect ratios of EMAA-1 and EMAA-2-based nanocomposites compared to the LDPE nanocomposite. It is interesting to note that there is no significant change in the filler particle dimensions when the methacrylic acid content is increased from 3.9 wt% to 8.9 wt%. Nanocomposites prepared from the ionomer had the largest particle aspect ratio, which suggests that of the four polymers, the ionomer is the most effective at exfoliating the $M_2(HT)_2$ organoclay. As mentioned in Table 1, the ionomer used in this study contains 15.2 wt% methacrylic acid, of which 40% is neutralized with sodium acetate to form a sodium salt, i.e., it contains ~9 wt% of unneutralized methacrylic acid (similar to EMAA-2) with ~6 wt% of neutralized acid. Unfortunately, it is not possible to identify the precise contribution of each components (unneutralized and neutralized methacrylic acid groups and sodium ion clusters) of the ionomer to this result.

5. Comparison with Halpin–Tsai model

Numerous attempts have been made to model the properties of nanocomposites and to correlate the experimental data with such models [21,34–36]. In most cases, modeling is carried out based on the assumption of fully exfoliated and well-oriented clay layers. However, in this study the morphology of the nanocomposites shows a wide range of diversity – mostly unexfoliated for LDPE-based nanocomposites to fairly exfoliated for ionomer-based nanocomposites. Hence, it would not be appropriate to model all the composites in the same way. To account for these differences, we model the ionomer-based nanocomposite as an exfoliated nanocomposite (not an unreasonable assumption considering the evidence provided by TEM micrographs in Fig. 7) and the composites prepared from LDPE, EMAA-1, and EMAA-2 as partially exfoliated composites in which the partially exfoliated organoclay particle can be treated as the filler particle as previously suggested by Fornes and Paul [21]. The tensile modulus of such a filler particle (E_p) in the direction parallel to the long axis of the particle (and individual MMT platelets) can be estimated by using the rule of mixtures, as described by Brune and Bicerano [37]

$$E_p = v_{MMT}E_{MMT} + v_{gallery}E_{gallery} \quad (1)$$

where, v_{MMT} and $v_{gallery}$ are the volume fractions of the montmorillonite platelet (in a particle) and the gallery space, respectively, while E_{MMT} and $E_{gallery}$ are their corresponding moduli. Since, the modulus of the platelet is significantly larger than the modulus of the gallery, Eq. (1) reduces to

$$E_p = v_{MMT}E_{MMT} \quad (2)$$

The volume fraction of the montmorillonite platelets within a particle was determined using the d-spacing of pure MMT ($d_{001} = 0.96$ nm) and of the nanocomposites obtained from WAXD analysis of the samples. For example, the X-ray scans of LDPE–$M_2(HT)_2$ nanocomposites reveal a d-spacing of 2.25 nm (see Fig. 4). Hence, $v_{MMT} \sim 0.96/2.25 = 0.427$, which when substituted in Eq. (2) gives the tensile modulus of the filler particle as 76 GPa. The tensile moduli of the particles were then inserted in the analytical form of the Halpin–Tsai model [32,33,38,39]

$$\frac{E}{E_m} = \frac{1 + \zeta\eta\phi_f}{1 - \eta\phi_f} \quad (3)$$

where ϕ_f is the volume fraction of the filler, ζ is a shape parameter which could be approximated as $2 \times$ (particle aspect ratio) [39], and η is given by

$$\eta = \frac{E_p/E_m - 1}{E_p/E_m + \zeta} \quad (4)$$

The values of the modeling parameters for all nanocomposites containing 2.5 wt% MMT prepared using $M_2(HT)_2$ organoclay are included in Table 4. As mentioned earlier, the

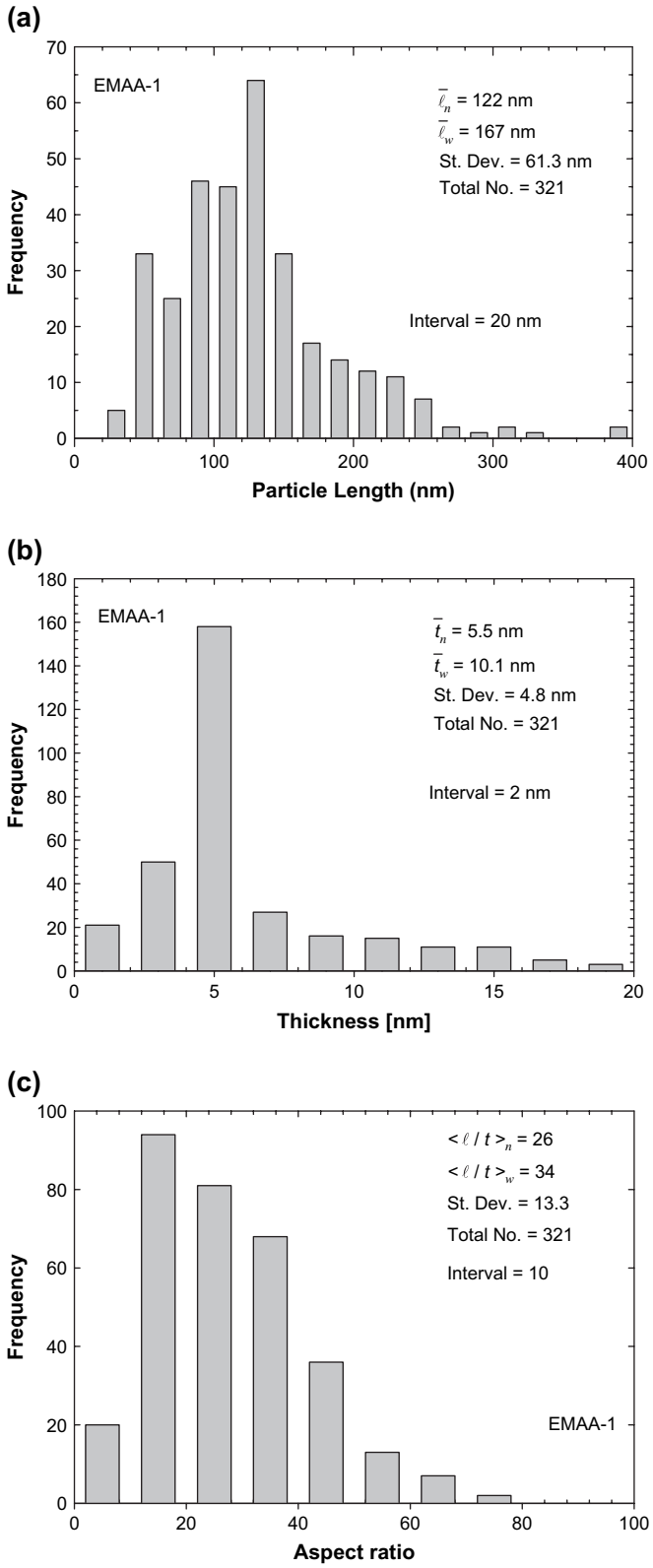

Fig. 10. Histograms of filler (a) particle length, (b) thickness, and (c) aspect ratio obtained by analyzing TEM micrographs of nanocomposites containing ~2.5 wt% MMT prepared from $M_2(HT)_2$ organoclay and ethylene/methacrylic acid copolymer, EMAA-1.

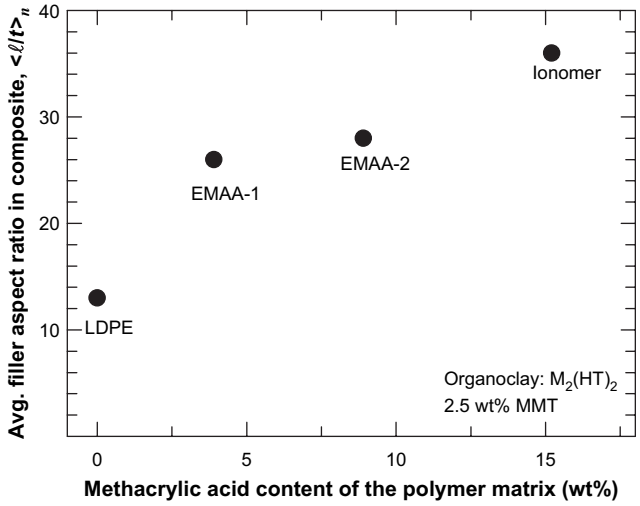

Fig. 11. Filler particle aspect ratio of nanocomposites containing 2.5 wt% MMT ($M_2(HT)_2$ organoclay) plotted as a function of the methacrylic acid content of the corresponding matrix polymers. The abscissa has been extended beyond zero for clarity.

ionomer-based nanocomposite is modeled as an exfoliated system where $E_p = 178$ GPA, the modulus of MMT. The above equations were used to derive the filler aspect ratio of nanocomposites for a given value of E/E_m.

The results deduced from the model are compared with experimental data in Fig. 12. As is evident, none of the four averages shows complete agreement (i.e. for all four polymers) with the values deduced from the model. For example, the experimentally determined number-average aspect ratio of filler particles, $\langle \ell/t \rangle_n$, for nanocomposites formed from LDPE and the ionomer shows good agreement with the theoretically derived values. However, for both EMAA copolymers the same average ($\langle \ell/t \rangle_n$) shows significant disagreements with the aspect ratios deduced from the model. Thus, it is difficult to say which statistical average best represents the nanocomposites examined in this study, i.e., which average should be used for modeling calculations. Of course, it should be remembered that numerous assumptions are built into the calculations based on the Halpin–Tsai model [32,33,38,39]. The particle analysis method used also has a few practical

Table 4
Parameters used for Halpin–Tsai modeling[a]

	d-spacing (d_{001}, Å)	Vol. fraction of MMT in a particle (v_{MMT})	Modulus of particle (E_p, Gpa)	E_p/E_m	Vol. fraction of the filler in nanocomposite (ϕ_f)
LDPE	2.25	0.427	76.0	666.7	0.0192
EMAA-1	2.42	0.397	70.6	598.3	0.0209
EMAA-2	2.76	0.348	61.9	847.9	0.0239
Ionomer	NA	1	178.0	679.4	0.0086

[a] Nanocomposites contained 2.5 wt% MMT and were prepared using $M_2(HT)_2$ organoclay. Ionomer-based nanocomposite was modeled as an exfoliated composite whereas composites prepared from LDPE, EMAA-1, and EMAA-2 were modeled as partially exfoliated composites.

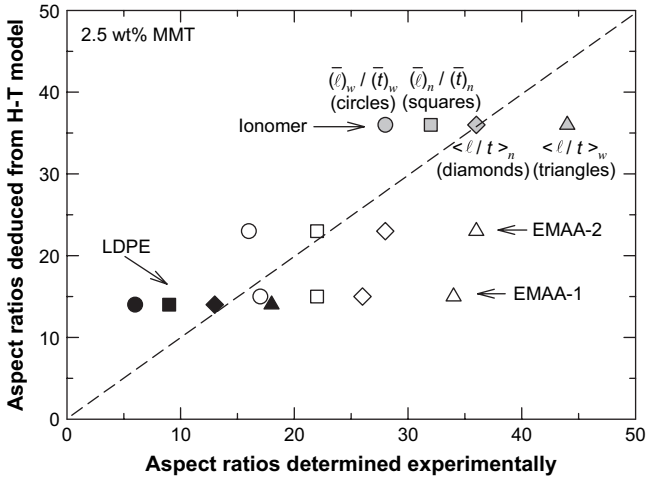

Fig. 12. Comparison between the experimentally determined particle aspect ratios of nanocomposites and their theoretical values deduced from Halpin–Tsai (H–T) model. The nanocomposites contain 2.5 wt% MMT and were prepared using $M_2(HT)_2$ organoclay.

limitations associated with it as described in earlier papers [9,30].

6. Conclusion

Mechanical properties and morphologies of nanocomposites prepared by melt mixing organoclays with LDPE, ethylene/methacrylic acid copolymers, and a sodium ionomer of poly(ethylene-*co*-methacrylic acid) were compared to evaluate the effects of matrix modification on the exfoliation efficiency of LDPE. With all four polymers, the use of a two-tailed organoclay, $M_2(HT)_2$, led to the formation of more exfoliated nanocomposites than a one-tailed organoclay, $M_3(HT)_1$. Nanocomposites prepared from EMAA copolymers revealed higher levels of organoclay exfoliation compared to equivalent composites prepared from LDPE. Of the four polymers, the ionomer-based nanocomposites exhibited the most exfoliated morphology. However, it was difficult to conclude whether this is a result of its higher methacrylic acid content or the fact that some of the acid units in the ionomer have been neutralized to form a salt with possibly different interactions between the organoclay and the acid units present in the polymer.

These results warrant a more extended study using custom designed EMAA copolymers and ionomers such that the two polymers have the same acid contents and melt indices. Such polymers are challenging to make since neutralization dramatically affects the rheology [16,40,41]. However, such a comparison would help to identify the precise role played by the ionic units versus acid units on organoclay exfoliation.

Acknowledgements

The authors sincerely thank Doug Hunter and Tony Gonzales of Southern Clay Products, Inc. for providing organoclay materials, WAXS data, and many helpful discussions.

References

[1] Lee H-S, Fasulo PD, Rodgers WR, Paul DR. Polymer 2005;46(25):11673–89.
[2] Hotta S, Paul DR. Polymer 2004;45(22):7639–54.
[3] Hasegawa N, Kawasumi M, Kato M, Usuki A, Okada A. Journal of Applied Polymer Science 1998;67(1):87–92.
[4] Hasegawa N, Okamoto H, Kawasumi M, Kato M, Tsukigase A, Usuki A. Macromolecular Materials and Engineering 2000;280(281):76–9.
[5] Li X, Wang C-y, Fang L, Liu L-z. Harbin Ligong Daxue Xuebao 2003;8(2):90–3.
[6] Rose J. Modern Plastics, vol. 37; October 2001.
[7] Garces JM, Moll DJ, Bicerano J, Fibiger R, McLeod DG. Advanced Materials (Weinheim, Germany) 2000;12(23):1835–9.
[8] Editors. Modern Plastics Worldwide 2005;82(9):48–50.
[9] Shah RK, Cui L, Williams KL, Bernard B, Paul DR. Journal of Applied Polymer Science 2006;102(3):2980–9.
[10] Filippi S, Marazzato C, Magagnini P, Minkova L, Dintcheva NT, La Mantia FP. Macromolecular Materials and Engineering 2006;291(10):1208–25.
[11] Cser F, Bhattacharya SN. Journal of Applied Polymer Science 2003;90(11):3026–31.
[12] Zhang Wa, Chen D, Zhao Q, Fang Ye. Polymer 2003;44(26):7953–61.
[13] Tang Y, Hu Y, Wang J, Zong R, Gui Z, Chen Z, et al. Journal of Applied Polymer Science 2004;91(4):2416–21.
[14] La Mantia FP, Lo Verso S, Dintcheva NT. Macromolecular Materials and Engineering 2002;287(12):909–14.
[15] Alexandre M, Beyer G, Henrist C, Cloots R, Rulmont A, Jerome R, et al. Macromolecular Rapid Communications 2001;22(8):643–6.
[16] Eisenberg A, Kim J-S. Introduction to ionomers. New York: Wiley; 1998. p. 327.
[17] Fornes TD, Yoon PJ, Keskkula H, Paul DR. Polymer 2001;42(25):9929–40.
[18] Fornes TD, Yoon PJ, Hunter DL, Keskkula H, Paul DR. Polymer 2002;43(22):5915–33.
[19] Shah RK, Hunter DL, Paul DR. Polymer 2005;46(8):2646–62.
[20] Fornes TD, Yoon PJ, Paul DR. Polymer 2003;44(24):7545–56.
[21] Fornes TD, Paul DR. Polymer 2003;44(17):4993–5013.
[22] Chavarria F, Paul DR. Polymer 2004;45(25):8501–15.
[23] Fornes TD, Hunter DL, Paul DR. Macromolecules 2004;37(5):1793–8.
[24] Shah RK, Takahashi S, Krishnaswamy RK, Paul DR. Polymer 2006;47(17):6187–201.
[25] Uribe-Arocha P, Mehler C, Puskas JE, Altstadt V. Polymer 2003;44(8):2441–6.
[26] Ren J, Casanueva BF, Mitchell CA, Krishnamoorti R. Macromolecules 2003;36(11):4188–94.
[27] Shah RK, Paul DR. Polymer 2006;47(11):4075–84.
[28] Paul DR, Zeng QH, Yu AB, Lu GQ. Journal of Colloid and Interface Science 2005;292(2):462–8.
[29] Shah RK. Ph.D. Dissertation. The University of Texas at Austin; 2006.
[30] Shah RK, Paul DR. Macromolecules 2006;39(9):3327–36.
[31] Fornes TD, Paul DR. Macromolecules 2004;37(20):7698–709.
[32] Halpin JC, Finlayson KM, Ashton JE. Primer on composite materials analysis. 2nd rev./ed., vol. xi. Lancaster, PA: Technomic Pub. Co.; 1992. p. 227.
[33] Halpin JC, Kardos JL. Polymer Engineering and Science 1976;16(5):344–52.
[34] Sheng N. Ph.D. Dissertation, Massachusetts Institute of Technology; 2002.
[35] Sheng N, Boyce MC, Parks DM, Rutledge GC, Abes JI, Cohen RE. Polymer 2004;45(2):487–506.
[36] Lee KY, Paul DR. Polymer 2005;46(21):9064–80.
[37] Brune DA, Bicerano JU. Polymer 2002;43(2):369–87.
[38] Halpin JC. Journal of Composite Materials 1969;3:732–4.
[39] Ashton JE, Halpin JC, Petit PH. Primer on composite materials: analysis, vol. vi. Stamford, Connecticut: Technomic Pub. Co.; 1969. p. 124.
[40] Troeltzsch C. Dupont. Personal communication.
[41] Walsh DJ. Dupont. Personal communication.